

Document downloaded from:

<http://hdl.handle.net/10251/65405>

This paper must be cited as:

García Ivars, J.; Iborra Clar, Ml.; Alcaina Miranda, Ml.; Mendoza Roca, JA.; Pastor Alcañiz, L. (2016). Surface photomodification of flat-sheet PES membranes with improved antifouling properties by varying UV irradiation time and additive solution pH. *Chemical Engineering Journal*. 283:231-242. doi:10.1016/j.cej.2015.07.078.



The final publication is available at

<http://dx.doi.org/10.1016/j.cej.2015.07.078>

Copyright Elsevier

Additional Information

# **SURFACE PHOTOMODIFICATION OF FLAT-SHEET PES MEMBRANES WITH IMPROVED ANTIFOULING PROPERTIES BY VARYING UV IRRADIATION TIME AND ADDITIVE SOLUTION PH**

Jorge Garcia-Ivars\*<sup>a</sup>, Maria-Isabel Iborra-Clar<sup>a,b</sup>, Maria-Isabel Alcaina-Miranda<sup>a,b</sup>, José-Antonio Mendoza-Roca<sup>a,b</sup>, Laura Pastor-Alcañiz<sup>c</sup>

<sup>a</sup>Research Institute for Industrial, Radiophysical and Environmental Safety (ISIRYM), Universitat Politècnica de València, C/Camino de Vera s/n, 46022 Valencia, Spain

<sup>b</sup>Department of Chemical and Nuclear Engineering, Universitat Politècnica de València, C/Camino de Vera s/n, 46022 Valencia, Spain

<sup>c</sup>Depuración de Aguas de Mediterráneo (DAM), Avda. Benjamin Franklin, 21, Parque Tecnológico 46980 Paterna, Spain

Tel. +34 963879633

Fax. +34 963877639

Correspondence to: Jorge Garcia-Ivars (E-mail: [jorgariv@posgrado.upv.es](mailto:jorgariv@posgrado.upv.es))

## **ABSTRACT**

Different polyethersulfone ultrafiltration membranes modified using UV irradiation in the presence of additives with different nature: hydrophilic aluminium oxide (Al<sub>2</sub>O<sub>3</sub>) nanoparticles and organic polyethylene glycol (PEG). The influence of the additive concentration, the irradiation time and the pH of the additive solution on several membrane characteristics related to its antifouling properties were investigated. These properties were analysed by means of hydrophilicity measurements (water contact angle, degree of modification, water permeability, porosity, and pore size), surface microscopic techniques (ATR-FTIR, SEM and AFM) and cross-flow filtration experiments using industrial wastewaters (residual brines from table olive processing

wastewaters). Results showed that all the PES membranes modified with different PEG/Al<sub>2</sub>O<sub>3</sub> concentrations improved the hydrophilicity of the membrane, except for membranes modified at pH 7. In addition, superior antifouling properties were provided by PES membranes modified with nano-sized Al<sub>2</sub>O<sub>3</sub> at a concentration of 0.5 %, low irradiation time (10 min) and acidic pH values (about pH 3). Therefore, surface membrane modification via UV irradiation with hydrophilic compounds is an appropriate technique to improve membrane performance applied in certain industrial fields.

**KEYWORDS** hydrophilicity; antifouling properties; UV-induced surface modification; additive solution pH; polyethylene glycol/aluminium oxide nanoparticles.

## **1. INTRODUCTION**

Polyethersulfone (PES), a high temperature amorphous thermoplastic polymer, has been widely used in manufacturing asymmetric membranes due to its mechanical, thermal and chemical resistances [1,2]. Nevertheless, this polymer is fouled during aqueous filtration due to its low hydrophilic character. Over the past few years, many researchers have investigated different approaches to modify PES asymmetric membrane surfaces in order to minimise the fouling phenomena (both organic and inorganic) and their effects in the membrane performance during the filtration process [3,4].

Membrane fouling is one of the most serious, complex and inevitable problems during membrane separation processes, especially in ultrafiltration process. These phenomena consist of the adsorption and deposition of different solutes (such as particles, colloids, macromolecules, salts, and proteins) on the surface or inside the pores of a membrane.

The main effect of these phenomena is a dramatic and long-term permeate flux decline along all the membrane separation processes due to a reduction of pore dimensions caused by the solute sorption on the membrane pore walls and the formation of a cake and/or gel layer on the membrane surface [5]. As a consequence, productivity and selectivity are negatively affected and therefore, membrane lifetime is reduced [2].

Generally, surface governs the permselective properties of a membrane which indicates that its properties (such as hydrophobic/hydrophilic properties, zeta potential, surface roughness, porosity, pore size and distribution) are crucial in membrane lifetime due to the fact that the separation process and interactions between solute macromolecules and membrane materials occur on the surface [6]. For this purpose, the development of modification techniques is focused on improving the surface characteristics to minimise the undesired interactions described previously and to obtain high selectivity and permeability without modifying the mechanical properties of the pretreated membranes. All of these works have been published in several patents, articles, reviews, and books applied to different areas such as wastewater treatment, biomedical applications, drinking water production, removal of pharmaceuticals from wastewaters, and recovery of high-added-value products [7-9].

Recent studies are focused on developing antifouling PES membranes by modifying the surface using different methods such as interfacial polymerisation, coating a protective layer and UV-induced modification. Interfacial polymerisation is the most common method for commercial fabrication of thin-film composite (TFC) membranes, which consist of an amorphous, dense and ultra-thin layer on a microporous PES membrane. The polymerisation reaction occurs at interfacial boundary of two immiscible solutions,

usually a water soluble monomer and an organic soluble monomer, whereas a thin selective layer is deposited on the membrane surface using coating techniques without any chemical reaction. Therefore, a porous MF/UF membrane could be used for preparing NF membranes by using any of both methods [9]. UV-induced modification stands out among all the surface modification techniques developed to improve PES surface properties for many applications due to its simplicity, usefulness, versatility, and low cost, which make its use very widespread. Other researchers have demonstrated that all polyarylsulfone materials are intrinsically photosensitive at a wavelength higher than 254 nm [7,10]. Its main advantage is the ability to modify different properties on the PES surface by introducing functional groups from the selected monomer (or monomers) or by entrapping inorganic nanoparticles without affecting the bulk properties [7,11]. This method can be divided into UV-grafting process using monomers and UV-induced modification using nanoparticles.

In this work, nano-sized alumina ( $\text{Al}_2\text{O}_3$ ) is used as an additive to introduce hydrophilic inorganic nanoparticles on the membrane surface without modifying the PES matrix of the membrane. Inorganic nanoparticles have unique physicochemical properties compared to the characteristics from the bulk materials that form membranes. For this reason, nanoparticles are of high interest in membrane synthesis to control membrane fouling and to obtain desired structures and functionalities. Many types of nanoparticles have been studied to enhance the permselective properties of a membrane, such as carbon nanotubes (CNTs), zirconia ( $\text{ZrO}_2$ ), silica ( $\text{SiO}_2$ ), silver (Ag), titanium oxide ( $\text{TiO}_2$ ), zinc oxide (ZnO), and even  $\text{Al}_2\text{O}_3$  [6,12]. However, there are few studies about the use of nanoparticles to modify membranes by UV-induced modification. Rahimpour et al. (2008) investigated the influence of  $\text{TiO}_2$  nanoparticles on the separation

performance of PES membranes, where UV-irradiated PES/TiO<sub>2</sub> membranes presented higher flux and antifouling properties compared to those membranes made by phase-inversion method. The best results were obtained by UV-irradiated membranes formed by TiO<sub>2</sub> deposited on PES membranes [1]. Same authors studied the effect of TiO<sub>2</sub> nanoparticles added on the polyvinylfluoride/sulfonated polyethersulfone (PVDF/SPES) membrane via UV-irradiation, where the presence of nanoparticles improved its antifouling properties and also, its antibacterial property [13].

This research aimed to investigate the influence of nanoparticles on the performance of commercial PES membranes in order to improve their hydrophilicity, permeability and selectivity. The novelties of this work are to introduce Al<sub>2</sub>O<sub>3</sub> nanoparticles via UV irradiation because all the studies about this method use TiO<sub>2</sub> nanoparticles and also to study the influence of the pH of the additive solution on the membrane characteristics and performance. The effect of these nanoparticles in terms of morphology, permeability properties and membrane hydrophilicity was studied. Morphology and composition of each membrane were analysed by porosity, attenuated total reflection Fourier transform infrared spectroscopy (ATR-FTIR), scanning electron microscopy (SEM), and atomic force microscopy (AFM). Membrane hydrophilicity was determined using water contact angle measurements. Finally, membrane performances were tested by water permeation, molecular weight cut-off (MWCO) determination using different molecular weights of PEG, and fouling studies using table olive processing wastewaters (TOPW).

## **2. EXPERIMENTAL**

### *2.1. Materials*

Flat-sheet PES ultrafiltration membranes with a MWCO of 30 kDa were purchased from Synder Filtration (USA). Aluminium oxide nanoparticles in gamma phase with primary particle size of 13 nm and a surface area of 100 m<sup>2</sup>/g, and polyethylene glycol of 400 Da were used as additives during UV modification. Both chemicals were selected to study the effects of different organic/inorganic additives on the membrane performance and were supplied by Sigma Aldrich (Germany). Deionised water was used throughout this study unless otherwise indicated.

## *2.2. Membrane modification*

Commercial membranes were modified by UV light irradiation in the presence of additive solutions with different compositions. Surface modification equipment was described elsewhere [14]. Membranes were placed in a Petri dish and dipped in additive solutions formed by well-dispersed PEG/Al<sub>2</sub>O<sub>3</sub> nanoparticles in aqueous media. After 5 min, membrane samples were illuminated by UV light ( $\lambda \approx 300$  nm) for several irradiation times (10, 20 and 30 min, respectively) with an intensity of 30 mW/cm<sup>2</sup>. All the modification process was also controlled by fixing the relative humidity of the environment (40 %). Thereafter, membranes were taken out and rinsed with tap water to remove the unreacted compounds, and then were immediately washed with deionised water twice at room temperature for 30 min and in between them, one wash at 50 ± 2 °C for 2 h. Finally, all the modified membranes were stored in deionised water for at least 1 day until use. This modification process is similar to that used in other studies about photomodified membranes [14,15].

## *2.3. Membrane characterisation*

### *2.3.1. ATR-FTIR*

The chemical structures of the different modified membranes were confirmed by ATR-FTIR spectroscopic technique. ATR-FTIR spectra were recorded on a Thermo Nicolet® Nexus spectrometer equipped with an HATR accessory consisting of a flat plate ZnSe crystal at a nominal incident angle of 45 °, and a gripper device to achieve a better contact between the HATR crystal and the sample. For each measurement, 128 scans were performed for an operating range from 600 to 4000 cm<sup>-1</sup> with a resolution of 4 cm<sup>-1</sup>. Membranes were dried in a vacuum oven overnight at room temperature before analysis.

### 2.3.2. SEM

A scanning microscope (JEOL JSM6300, Japan) was employed for studying the cross-sectional morphology of all the modified membranes. For this purpose, SEM work was performed at an accelerating voltage of 20 keV in high vacuum conditions. Membranes were cut into small pieces and immersed in liquid nitrogen. Then, the frozen membrane samples were fractured and kept in air for drying. Dried samples were carbon sputtered to make them conductive, prior to SEM analyses.

### 2.3.3. AFM

Surface roughness of all modified membranes were further visualised by a tapping mode AFM (VEECO Instruments, United States). Images were obtained over different square areas of each membrane sample based on a scan area of around 5 µm x 5 µm. Roughness values were determined by averaging the values measured over 1 µm x 1 µm in ten different locations chosen arbitrarily for each membrane sample. The average roughness ( $S_a$ ) represents the mean value of the surface height relative to the calculated center plane, for which the volumes enclosed by the image above and below the plane

are the same. It was calculated by the following expression, in which the number of points within the given area ( $N_p$ ) considered was 512 data points:

$$S_a = \frac{1}{N_p} \sum_{i=0}^{N_p} |Z_i - Z_{avg}| \quad \text{Eq. (1)}$$

where  $Z_i$  is the current height value measured, while  $Z_{avg}$  is the average of the height values within the given area.

#### 2.3.4. Water contact angle

An OCA20 contact angle system (Dataphysics, Germany) was used for determining the water contact angle of each dried membrane surface. Contact angle measurements were performed by the sessile drop technique. 3  $\mu\text{L}$  of ultrapure water were dropped on each dried membrane sample from a microsyringe with a stainless steel needle at room-temperature conditions. Average of ten random locations was taken for each sample.

#### 2.3.5. Degree of modification

The degree of modification ( $DM$ ) of PEG/ $\text{Al}_2\text{O}_3$  nanoparticles on all membranes was gravimetrically determined by the following formula:

$$DM = \frac{(m_1 - m_0)}{A} \quad \text{Eq. (2)}$$

where  $m_0$  is the weight of the initial membrane sample,  $m_1$  is the weight of the modified membrane, and  $A$  is the active surface area of the membrane used. Each  $DM$  value was an average of at least three parallel experiments and all the samples used for  $DM$  determination were not used for flux and fouling experiments.

#### 2.3.6. Membrane porosity

The overall porosity ( $\varepsilon$ ) of membranes was determined by wet-dry weighting method and it was calculated as the volume of the pores divided by the total volume of the porous membrane [16]:

$$\varepsilon = \frac{\frac{(W_W - W_D)}{\rho_W}}{\frac{(W_W - W_D)}{\rho_W} + \frac{W_D}{\rho_p}} \quad \text{Eq. (2)}$$

where  $W_W$  is the weight of the wet membrane (g),  $W_D$  is the weight of the dry membrane (g),  $\rho_W$  is the density of pure water at operating conditions ( $\text{g/cm}^3$ ), and  $\rho_p$  is the density of the polymer ( $\text{g/cm}^3$ ).

## 2.4. Membrane performance

### 2.4.1. Water permeation

Water permeation properties of the modified membranes were tested using a standard cross-flow UF setup, which is described in an earlier paper [17]. Firstly, all the membranes were compacted for at least 30 min, 3 bar, 25 °C and a cross-flow velocity of 2.08 m/s. The water flux was generally stable after 30 min, when the difference between values of the permeate mass during the filtration time was lower than 2 %. After the compaction procedure, water permeability experiments were carried out with deionised water at different transmembrane pressures ( $\Delta P$ ) ranging from 1 to 3 bar at a constant flow rate of 300 L/h and 25 °C. The deionised water flux ( $J_W$ ,  $\text{L/m}^2 \cdot \text{h}$ ) was measured using the gravimetric method and was determined by:

$$J_W = \frac{V}{A_m \cdot t} \quad \text{Eq. (5)}$$

where  $V$  was the volume of permeate water ( $\text{m}^3$ ),  $A_m$  was the effective surface area of the membrane ( $\text{m}^2$ ) and  $t$  was the permeation time (h). So, water permeability ( $P_H$ ) was obtained from the slope of the plot of  $J_W$  and  $\Delta P$  and was calculated by

$$P_H = \frac{J_W}{\Delta P} \quad \text{Eq. (6)}$$

According to Darcy's law, the intrinsic resistance of the membrane ( $R_m$ ) was calculated using the following equation (Eq. (7)):

$$R_m = \frac{1}{\mu \cdot K_W} \quad \text{Eq. (7)}$$

#### 2.4.2. PEG rejection

PEG rejection tests were performed using the same above-mentioned UF system at a constant cross-flow velocity (2.08 m/s), 25 °C and  $\Delta P$  ranging from 0.5 to 4 bar. PEG solutions (molecular weight from 10 to 35 kDa) with a concentration of 1 g/L were prepared individually using deionised water and were used as the feed solution. PEG concentrations were analysed using a high-precision Atago Refractometer (Atago RX-5000) at 20 °C within an accuracy of  $\pm 0.00004$  units. The PEG rejection percentage ( $R_{peg}$ ) was calculated by the following expression:

$$R_{peg}(\%) = \left( 1 - \frac{C_p}{C_f} \right) \cdot 100 \quad \text{Eq. (8)}$$

where  $C_p$  is the PEG concentration in the permeate stream and  $C_f$  is the PEG concentration in the feed solution.

The surface pore radius was calculated based on the next equation [18]:

$$r_m(m) = 16.73 \cdot 10^{-12} \cdot M_w^{0.557} \quad \text{Eq. (9)}$$

where  $M_w$  is the PEG molecular weight (Da).

#### 2.4.3. Fouling study

In order to compare the biofouling on the unmodified and photomodified membranes, residual brines from table olive processing were used as feed solution and their main physicochemical characteristics are summarised in Table 1. The acidity of this effluent and both high salt and organic concentration are the most important properties of this wastewater (TOPW). Each membrane was initially compacted with deionised water in the above-mentioned UF experimental setup for 30 min at 2 bar and constant cross-flow velocity (2.08 m/s). After that, a fouling step was performed to check the antifouling properties of all the membranes at 2 bar for 2 h. The permeate flux  $J_f$  ( $L/m^2 \cdot h$ ) was measured by gravimetric method. Normalised flux ratio (*NFR*) was defined as the ratio between the membrane flux at the beginning and at the end of the fouling process ( $J_{f1}$  and  $J_{f2}$ , respectively), and it was determined as follows:

$$NFR(\%) = \left( \frac{J_{f2}}{J_{f1}} \right) \cdot 100 \quad \text{Eq. (10)}$$

This parameter was used to evaluate the fouling-resistant capability of all the membranes tested and higher *NFR* values (next to 1) indicate better antifouling property of a membrane.

### 3. RESULTS AND DISCUSSION

#### 3.1 Membrane characterisation

Twelve different membranes were photomodified with different additive concentrations, UV irradiation times and the pH of additive solutions (or additive solution pH). The characteristics for each flat-sheet PES membrane tested are presented in Table 2. When the membrane surface was irradiated by UV light ( $\lambda \approx 300$  nm), free radicals were generated in several sites on the surface and on the pore walls, because PES material is intrinsically photosensitive. These free radicals reacted with PEG present in the additive

solution and Al<sub>2</sub>O<sub>3</sub> nanoparticles were deposited and physically entrapped on the nascent surface structure due to the polymerisation reactions between PES and PEG compounds. In order to confirm the success of the modification process and provide information about the surface chemistry of each membrane before and after modification was analysed using ATR-FTIR analysis. Fig. 1 depicts the ATR-FTIR spectra of the photomodified PES membrane surfaces with different compositions, irradiation times and additive solution pHs. The effects of the additive composition and the irradiation time on the modified surface were shown in Fig. 1(a), where new absorption peaks appeared in ATR-FTIR spectra of the photomodified membranes in comparison with those obtained for the control PES membrane. Firstly, the characteristic broad band appeared at 3300-3400 cm<sup>-1</sup> increased its intensity when both additives (PEG and Al<sub>2</sub>O<sub>3</sub>) were incorporated on the membrane surface, due to the presence of both hydrated Al<sub>2</sub>O<sub>3</sub> and O-H groups from grafted PEG chains [15,19]. A new absorption peak was observed at 1645 cm<sup>-1</sup>, which could be assigned to the carboxyl group in asymmetric stretching and it appeared when PES material is irradiated using UV light. Three small absorption peaks also appeared at 623, 795 and 1080 cm<sup>-1</sup> could be attributed to the stretching vibrations and symmetric bending modes of Al-O-Al bonds, which evidenced the presence of Al<sub>2</sub>O<sub>3</sub> nanoparticles on the membrane surface. In the same way, the ether group from PEG appeared at the same wavelength of this last absorption peak, which indicates that the analytical peak at 1080 cm<sup>-1</sup> in PES/PEG/Al<sub>2</sub>O<sub>3</sub> membranes could be assigned to the sum of the presence of ether group and the Al-O-Al bond contributions [15,20]. All these absorption peaks confirmed the success of the modification process.

The influence of the irradiation time on the modification process is depicted in Fig. 1(a), where longer irradiation times caused a slight increase in the intensity of the absorption bands related to the presence of both additives. Thus, no significant differences were observed in ATR-FTIR spectra when the irradiation time varied. Fig. 1(b) shows the effect of different pHs of the additive solution during the modification process. Similar ATR-FTIR spectra were obtained at acidic and basic pHs. Compared to these ATR-FTIR spectra, lower intensities in all the absorption peaks related to the presence of additives were much lower when the pH of the additive solution was 7, principally due to the fact that the  $\text{Al}_2\text{O}_3$  nanoparticles were in the point of zero charge at these conditions, which favoured the formation of nanoparticle agglomerations and inherently caused a heterogeneous distribution of these nanoparticles on the surface. This behaviour will be explained in detail in AFM results.

The effect of different concentrations of PEG/ $\text{Al}_2\text{O}_3$  nanoparticles, additive solution pHs and UV irradiation times on the membrane morphology can be observed using SEM and AFM analyses. Fig. 2 presents the SEM images of the cross-sections obtained for each photomodified PES membrane and the unmodified control membrane. All the membranes had the typical structure of a flat-sheet membrane made by phase-inversion method: an asymmetric structure consisting of a dense thin skin layer, a porous thick open finger-like sublayer and the nonwoven support [5]. According to the SEM images of PES2-10 and PES2-30, an increasing in UV irradiation times resulted in more reaction time and then, the skin layer is denser compared to the control PES membrane (PES0). These results are in accordance with those obtained by Mansourpanah and Momeni Habili (2013), which demonstrated that longer UV irradiation times led to enhance the polymerisation degree and then obtain a denser thin layer [21]. It can also

be observed that the asymmetric structure was weakened, which was suffered deterioration after being exposed to high irradiation times (PES2-30), obtaining irregular pore channels. This could be caused by the formation of too many aggregated radicals on the membrane surface. The same deterioration was seen in PES1-30 (SEM image not shown) and it has been confirmed by other researchers [1]. The degradation of PES surface structure could be avoided at longer UV wavelength ( $\lambda \geq 350$  nm). As regards the influence of the additive solution pH, no significant differences were observed for all the photomodified membranes at different pH values. In the same way, there was no evidence of significant differences between the cross-section morphologies from membranes with different PEG/Al<sub>2</sub>O<sub>3</sub> concentrations (PES2-10 and PES3).

Fig. 3 provides the three-dimensional AFM images for all the membranes tested, with and without photomodification. The dark areas represent the surface pores of a membrane sample and the brightest regions are its highest points. From AFM images, it can be observed that the unmodified PES membrane had a very homogeneous smooth surface. All the photomodified membranes presented rougher surfaces than the unmodified PES surface, except those membranes that were modified at acidic pH using Al<sub>2</sub>O<sub>3</sub> nanoparticles and those membranes photomodified with PEG/Al<sub>2</sub>O<sub>3</sub> at low irradiation times. These results could be confirmed with the surface roughness, which was expressed in terms of mean roughness parameter ( $S_a$ ) and was shown in Table 3. This parameter barely increased from 1.1 to 1.2 nm when Al<sub>2</sub>O<sub>3</sub> was added. At pHs 3 and 10,  $S_a$  slightly changed (1.9 and 2.6 nm, respectively). However, when the pH in the additive solution was 7, rougher surface was obtained (5.7 nm). This behaviour could be explained by the uneven dispersion of these nanoparticles in the additive solution and also, on the surface after the modification process due to the agglomerations of Al<sub>2</sub>O<sub>3</sub>

nanoparticles formed at these conditions. As other researchers reported, the zero-point-of-charge of  $\text{Al}_2\text{O}_3$  is about pH 7, in which  $\text{Al}_2\text{O}_3$  nanoparticles have neutral or zwitterionic charge and thus, the maximum electrostatic attraction occurs among them [22]. Yoo *et al.* (2007) also demonstrated that  $\text{Al}_2\text{O}_3$ /water mixtures could suppress the Van der Waals interaction and therefore, could hinder the formation of agglomerations or clusters at basic pH. They also observed an increase in the number of agglomerations at pH 7 [23]. At longer irradiation times, rougher surfaces were achieved. This could be related to the higher incorporation of additive on the surface, the photosensitivity of PES and its higher degradation explained in SEM results. Higher presence of additives on the surface can also be observed at high additive concentration, which made the surface rougher during the reactions generated by UV irradiation.

Water contact angle is the most common parameter to evaluate the hydrophilic-hydrophobic properties of a membrane surface. Fig. 4 shows the effect of the additive concentration on the water contact angle measurements. The unmodified PES membranes exhibited the highest water droplet contact angle of all the membranes tested, with a value of about  $77^\circ$ . This value confirmed the semi-hydrophobic character of this material and is in accordance with the studies of other researchers [24]. These results indicated that incorporation of  $\text{Al}_2\text{O}_3$  nanoparticles could substantially increase the membrane hydrophilicity (by decreasing the contact angle), obtaining water contact angle values of about  $64^\circ$  at high  $\text{Al}_2\text{O}_3$  concentrations. This could be explained by the higher affinity of  $\text{Al}_2\text{O}_3$  for water molecules than PES. Additionally, an increase in membrane hydrophilicity could be related to a rougher surface, which implied a higher presence of  $\text{Al}_2\text{O}_3$  nanoparticles on the surface. The same trend was observed when PEG content increased in the additive solution, but the water contact angle obtained at

high PEG concentration ( $\sim 61.5^\circ$ ) was similar to those obtained for high  $\text{Al}_2\text{O}_3$  concentrations ( $\sim 64^\circ$ ). This means  $\text{Al}_2\text{O}_3$  nanoparticles were the main responsible for the improvement in membrane surface hydrophilicity in PES membranes photomodified with PEG/ $\text{Al}_2\text{O}_3$  nanoparticles.

Fig. 5 shows the influence of the additive solution pH and irradiation time on the water contact angle measurements. It can be observed in Fig. 5(a) a strong parabolic relationship between pH and water contact angle, achieving its maximum value at pH 7 ( $\sim 69^\circ$ ). This may be caused by the formed  $\text{Al}_2\text{O}_3$  agglomerations and clusters and their irregular dispersion on the surface at these conditions (as was explained in AFM section). The best conditions to obtain a hydrophilic membrane with  $\text{Al}_2\text{O}_3$  nanoparticles were at acidic pH ( $\sim 63.5^\circ$ ). The effect of irradiation time on the water contact angle is depicted in Fig. 6(b), where longer irradiation times implied lower contact angle values, especially for PES/ $\text{Al}_2\text{O}_3$  membranes. This could be explained by the incorporation of more additive content on the membrane surface when was exposed for longer irradiation times.

Table 3 summarises the results of the degree of modification for each membrane tested. It can be observed that the degree of modification was higher with increasing PEG/ $\text{Al}_2\text{O}_3$  content, especially with the presence of PEG. The combined effect of both additives during the UV irradiation modified the weight of the membrane incorporating these additives via graft polymerisation (PEG chains) and physically entrapment ( $\text{Al}_2\text{O}_3$ ). The free radicals generated in many sites on the PES surface by the UV irradiation reacted with the PEG chains from the additive solution, which could favour the entrapment of hydrophilic  $\text{Al}_2\text{O}_3$  nanoparticles on the surface structure. The same

trend was observed at higher irradiation time. However, the degree of modification during 30 min of irradiation time was slightly higher than those obtained for 20 min. This fact could be explained by the surface deterioration and degradation of PEG after being exposed for longer irradiation times [19,25]. The incorporation of Al<sub>2</sub>O<sub>3</sub> nanoparticles through UV-induced surface modification at different additive solution pH gave very similar values of degree of modification in all membranes, except the low value obtained for membranes at pH 7. This may be explained by the formed Al<sub>2</sub>O<sub>3</sub> agglomerations at these conditions, which could hinder their entrapment on the surface structure (as was explained above).

Fig. 6 shows the change in membrane porosity in terms of additive concentration. The incorporation of additives onto PES surface structure resulted in higher values of the overall porosity of the membranes. This increment was dramatically when PEG concentration increased (from 34 to 54 %), which demonstrated that the addition of PEG/Al<sub>2</sub>O<sub>3</sub> mixtures improved the porosity and then, the hydrophilic character of PES membranes. These results could be related to the rougher surfaces obtained for photomodified membranes and the decrease in their water contact angle values. Furthermore, this parameter is intimately related to the equilibrium water content [26]. Pulat and Babayigit (2001) demonstrated a strong straightforward relationship between equilibrium water content (and therefore, porosity) and the degree of modification by swelling measurements [27]. For these reasons, overall membrane porosity and degree of modification are also related. However, the presence of high Al<sub>2</sub>O<sub>3</sub> content barely affected the overall porosity of the PES/Al<sub>2</sub>O<sub>3</sub> membranes. Fig. 7 provides the results obtained for different additive solution pHs and irradiation times. In the first case, all the porosity values were similar to each other, regardless of the pH of the additive

medium (Fig. 7 (a)). The lowest value obtained for membrane porosity was that obtained for PES membranes photomodified at pH 7 (~ 38 %), which corresponded to PES membranes with the highest contact angle value obtained. With increasing the irradiation time, higher values of membrane porosity could be achieved, especially when the additive incorporated onto the PES membrane was PEG/Al<sub>2</sub>O<sub>3</sub> mixtures due to the hydrophilic character of the combination of both compounds (see Fig. 7 (b)).

### *3.2 Filtration experiments*

The effect of additive concentration on water permeability is depicted in Fig. 6. When additive was added on the surface, the water permeability decreased principally because both grafting and UV-induced modification reduced the pore size and thus water permeability decreased [28]. These results may be attributed to the higher degree of modification obtained at high additive concentrations, and also could be confirmed with the PEG rejection experiments, which calculated results are summarised in Table 3. The reduction in pore size after UV-induced surface modification was clearly observed, especially at high additive concentration (from 5.2 to 4.3 nm for PES/Al<sub>2</sub>O<sub>3</sub> membranes, and from 5.2 to 4.4 nm for PES/PEG/Al<sub>2</sub>O<sub>3</sub> membranes). There was also a change in water permeability for PES membranes after surface modification at different additive solution pH. These results are shown in Fig. 7 (a). At acidic pH, PES/Al<sub>2</sub>O<sub>3</sub> membranes presented similar values. But, when pH was 7, the water permeability increased up to similar values (~ 129 L/m<sup>2</sup>·h·bar) to those obtained for the unmodified PES membranes (~ 147 L/m<sup>2</sup>·h·bar). This effect could be caused by the heterogeneous dispersion of Al<sub>2</sub>O<sub>3</sub> nanoparticles on the surface structure and the agglomerations formed at these conditions. This heterogeneous dispersion resulted in the formation of an irregular surface with some parts of high hydrophilicity and roughness and others degraded by

the UV irradiation (as explained in AFM section). This was also reflected in the lower degree of modification obtained for this membrane (PES1-pH7). However, water permeability dramatically decreased at basic pH, where the  $\text{Al}_2\text{O}_3$  nanoparticles were not well-dispersed onto the surface in these conditions, obtaining a rougher and hydrophilic surface with lower pore size (4.2 nm). This could be caused by the presence of  $\text{Al}_2\text{O}_3$  nanoparticles deposited inside the surface pores during the modification process, plugging the pores of the PES membrane [29]. Regarding the results obtained for different irradiation times (Fig. 7 (b)), water permeability decreased at higher irradiation times due to the greater incorporation of hydrophilic additives onto the original PES membrane. This effect was similar to those obtained for membranes with increasing UV irradiation energy during the modification process performed by other researchers [28]. The pore size was barely affected by the UV irradiation time (see Table 3).

Finally, normalised flux ratio (*NFR*) was used to evaluate the fouling degree of the membranes. The evolution of this parameter with filtration time for PES/ $\text{Al}_2\text{O}_3$  membranes was shown in Fig. 8. It can be observed that almost all the photomodified membranes exhibited higher resistance towards fouling (higher *NFR* values) than the unmodified membrane (~ 52 %), except for PES1-30, PES1-pH7 and PES1-pH10. These results could be related to the high surface roughness obtained for these membranes, the heterogeneous dispersion of the  $\text{Al}_2\text{O}_3$  nanoparticles on the surface structure and even the degradation of PES material and its properties during the modification process. PES1-pH3 suffered the lowest total flux loss during the TOPW ultrafiltration and achieved the highest *NFR* values (~ 67 %). The performance of this membrane was followed by PES1-10 (PES/ $\text{Al}_2\text{O}_3$  membrane modified at pH 5), which

indicated that the best modification was obtained for PES membranes with  $\text{Al}_2\text{O}_3$  nanoparticles at acidic pH values and an irradiation time of 10 min. This conclusion is confirmed by comparing these results with those obtained for PES/PEG/ $\text{Al}_2\text{O}_3$  membranes (shown in Fig. 9). In this case, all the membranes photomodified in the presence of PEG/ $\text{Al}_2\text{O}_3$  nanoparticles showed higher *NFR* values than the unmodified membrane, which is an indicator of the successful alteration of the surface properties. PES2-10 membrane showed the highest resistance towards fouling among all the PES/PEG/ $\text{Al}_2\text{O}_3$  membranes. However, the performances of these membranes were worse than that showed for the PES/ $\text{Al}_2\text{O}_3$  membranes above mentioned. Furthermore, longer irradiation times reduced the antifouling properties of the membranes tested using both additives, showing the worst results for membranes modified at 30 min of irradiation time. These results can be seen in both Fig. 8 and 9. Finally, the effect of high additive concentrations on the membrane performance showed that there is a certain additive concentration at which the maximum fouling resistance could be achieved and further incorporation of this additive was counterproductive [30]. This effect was observed for both additives in Fig. 8 and 9, regardless their nature. For all these reasons, PES membranes modified via UV-irradiation for 10 min in the presence of  $\text{Al}_2\text{O}_3$  nanoparticles (in absence of PEG) at acidic pH values reported better *NFR* results and then, better antifouling properties.

#### 4. CONCLUSIONS

In order to obtain a high hydrophilic membrane with good antifouling properties, PES membranes were modified by UV-induced surface modification in the presence of different concentrations of two hydrophilic additives: a water-soluble monomer (PEG) and a metal oxide ( $\text{Al}_2\text{O}_3$ ). The degree of modification increased with additive

concentration. ATR-FTIR spectra, SEM and AFM analyses confirmed the incorporation of these additives on the PES surface structure. Also, water contact angle measurements corroborated that the hydrophilicity of photomodified membranes was improved compared with the unmodified membrane. Such increment in hydrophilicity, combined with the reduction of the pore size caused by the modification process, was an indicator of the improvement of membrane selectivity. Water permeability decreased after modification for all the membranes tested. Longer irradiation times degraded the polymer material and negatively affected the incorporation of additives onto the PES surface, especially for PES/Al<sub>2</sub>O<sub>3</sub> membranes. The pH of the additive solution proved to be a key parameter to obtain a successful modification using Al<sub>2</sub>O<sub>3</sub> nanoparticles at different pH values of 7, at which Al<sub>2</sub>O<sub>3</sub> nanoparticles formed agglomerations or clusters at these conditions. Furthermore, PES membranes modified with PEG/Al<sub>2</sub>O<sub>3</sub> nanoparticles improved their antifouling properties, especially for 0.5 wt% Al<sub>2</sub>O<sub>3</sub>/PES membranes exposed to UV irradiation during 10 min at acidic conditions.

## **5. ACKNOWLEDGEMENTS**

The authors of this work thank the financial support of CDTI (Centre for Industrial Technological Development) depending on the Spanish Ministry of Science and Innovation. The authors also thank the Center for Biomaterials and Tissue Engineering and the Electron Microscopy Service both from the Universitat Politècnica de València.

## **6. REFERENCES**

[1] Rahimpour, A., Madaeni, S.S., Taheri, A.H., Mansourpanah, Y., Coupling TiO<sub>2</sub> nanoparticles with UV irradiation for modification of polyethersulfone ultrafiltration membranes, *Journal of Membrane Science* 313 (2008) p. 158-169.

- [2] Yu, L., Zhang, Y., Zhang, B., Liu, J., Zhang, H., Song, C., Preparation and characterization of HPEI-GO/PES ultrafiltration membrane with antifouling and antibacterial properties, *Journal of Membrane Science* 447 (2013) p. 452-462.
- [3] Razmjou, A., Mansouri, J., Chen, V., The effects of mechanical and chemical modification of TiO<sub>2</sub> nanoparticles on the surface chemistry, structure and fouling performance of PES ultrafiltration membranes, *Journal of Membrane Science* 378 (2011) p. 73-84.
- [4] Peyravi, M., Rahimpour, A., Jahanshahi, M., Javadi, A., Shockravi, A., Tailoring the surface properties of PES ultrafiltration membranes to reduce the fouling resistance using synthesized hydrophilic copolymer, *Microporous and Mesoporous Materials* 160 (2012) p. 114-125.
- [5] Mulder, M. *Basic principles of membrane technology*, 2003, Kluwer Academic, Dordrecht, The Netherlands.
- [6] Kochkodan, V., Hilal, N., A comprehensive review on surface modified polymer membranes for biofouling mitigation, *Desalination* 356 (2015) p. 187-207.
- [7] Nady, N., Franssen, M.C.R., Zuilhof, H., Mohy Eldin, M.S., Boom, R., Schroën, K., Modification methods for poly(arylsulfone) membranes: a mini-review focusing on surface modification, *Desalination* 275 (2011) p. 1-9.
- [8] Ahmad, A.L., Abdulkarim, A.A., Ooi, B.S., y Ismail, S., Recent development in additives modifications of polyethersulfone membrane for flux enhancement, *Chemical Engineering Journal* 223 (2013) p. 246-267.
- [9] Zhao, C., Xue, J., Ran, F., Sun, S., Modification of polyethersulfone membranes – a review of methods, *Progress in Materials Science* 58 (2013) p. 76-150.

- [10] Norrman, K., Kingshott, P., Kaeselev, B., Ghanbari-Siahkali, A., Photodegradation of poly(ether sulphone) Part 1. A time-of-flight secondary ion mass spectrometry study, *Surface and Interface Analysis* 36 (2004) p. 1533-1541.
- [11] Ng, L.Y., Ahmad, A., Mohammad, A.W., Alteration of polyethersulphone membranes through UV-induced modification using various materials: a brief review, *Arabian Journal of Chemistry* (2013) <http://dx.doi.org/10.1016/j.arabjc.2013.07.009>
- [12] Ng, L.Y., Mohammad, A.W., Leo, C.P., Hilal, N., Polymeric membranes incorporated with metal/metal oxide nanoparticles: a comprehensive review, *Desalination* 308 (2013), p. 15-33.
- [13] Rahimpour, A., Jahanshahi, M., Mollahosseini, A., Rajaeian, B., Structural and performance properties of UV-assisted TiO<sub>2</sub> deposited nano-composite PVDF/SPES membranes, *Desalination* 285 (2012) p. 31-38.
- [14] García-Ivars, J., Alcaina-Miranda, M.I., Iborra-Clar, M.I., Mendoza-Roca, J.A., Pastor-Alcañiz, L., Development of fouling-resistant polyethersulfone ultrafiltration membranes via surface UV photografting with polyethylene glycol/aluminum oxide nanoparticles, *Separation and Purification Technology* 135 (2014) p. 88-99.
- [15] García-Ivars, J., Iborra-Clar, M.I., Alcaina-Miranda, M.I., Mendoza-Roca, J.A., Pastor Alcañiz, L., Treatment of table olive processing wastewaters using novel photomodified ultrafiltration membranes as first step for recovering phenolic compounds, *Journal of Hazardous Materials* 290 (2015) p. 51-59.
- [16] Luo, F., Zhang, J., Wang, X.L., Cheng, J.F., Xu, Z.J., Formation of hydrophilic EAA copolymer microporous membranes via thermally induced phase separation, *Acta Polymerica Sinica* (2002) p. 566-571.
- [17] García-Ivars, J., Alcaina-Miranda, M.I., Iborra-Clar, M.I., Mendoza-Roca, J.A., Pastor-Alcañiz, L., Enhancement in hydrophilicity of different polymer phase-inversion

ultrafiltration membranes by introducing PEG/Al<sub>2</sub>O<sub>3</sub> nanoparticles, *Separation and Purification Technology* 128 (2014) p. 45-57.

[18] Cheng, X.Q., Shao, L., Lau, C.H., High flux polyethylene glycol based nanofiltration membranes for water environmental remediation, *Journal of Membrane Science* 476 (2015) p. 95-104.

[19] Abednejad, A.S., Amoabediny, G., Ghaee, A., Surface modification of polypropylene membrane by polyethylene glycol graft polymerization, *Materials Science and Engineering C* 42 (2014) p. 443-450.

[20] Romero-Vargas Castrillón, S., Lu, X., Shaffer, D.L., Elimelech, M., Amine enrichment and poly(ethylene glycol) (PEG) surface modification of thin-film composite forward osmosis membranes for organic fouling control, *Journal of Membrane Science* 450 (2014) p. 331-339.

[21] Mansourpanah, Y., Momeni Habili, E., Preparation and modification of thin film PA membranes with improved antifouling property using acrylic acid and UV irradiation, *Journal of Membrane Science* 430 (2013) p. 158-166.

[22] Chen, W.R., *Interactions of tetracycline antibiotics with dissolved metal ions and metal oxides*. PhD Thesis, 2008, Georgia Institute of Technology (USA).

[23] Yoo, D.H., Hong, K.S., Hong, T.E., Eastman, Yang, H.S., Thermal conductivity of Al<sub>2</sub>O<sub>3</sub>/water nanofluids, *Journal of the Korean Physical Society* 51 (2007) 84-87.

[24] Balta, S., Sotto, A., Luis, P., Benea, Van der Bruggen, B., Kim, J., A new outlook on membrane enhancement with nanoparticles: the alternative of ZnO, *Journal of Membrane Science* 389 (2012) p. 155-161.

[25] Das, I., Gupta, S.K., Polyethylene glycol degradation by UV irradiation, *Indian Journal of Chemistry - Section A Inorganic, Physical, Theoretical and Analytical Chemistry* 44 (2005) p. 1355-1358.

- [26] Chakrabarty, B., Ghoshal A.K., Purkait, M.K., Effect of molecular weight of PEG on membrane morphology and transport properties, *Journal of Membrane Science* 309 (2008) p. 209-221.
- [27] Pulat, M., Babayigit, D., Surface modification of PU membranes by graft copolymerization with acrylamide and itaconic acid monomers, *Polymer Testing* 20 (2001) p. 209-216.
- [28] Emin, C., Remigy, J.C., Lahitte, J.F., Influence of UV grafting conditions and gel formation on the loading and stabilization of palladium nanoparticles in photografted polyethersulfone membrane for catalytic reactions, *Journal of Membrane Science* 455 (2014) p. 55-63.
- [29] Wei, X., Rong, W., Zhansheng, L., Fane, A.G., Development of a novel electrophoresis-UV grafting technique to modify PES UF membranes used for NOM removal, *Journal of Membrane Science* 273 (2006) p. 47-57.
- [30] Yune, P.S., Kilduff, J.E., Belfort, G., Fouling-resistant properties of a surface-modified poly(ether sulfone) ultrafiltration membrane grafted with poly(ethylene glycol)-amide binary monomers, *Journal of Membrane Science* 377 (2011) p. 159-166.

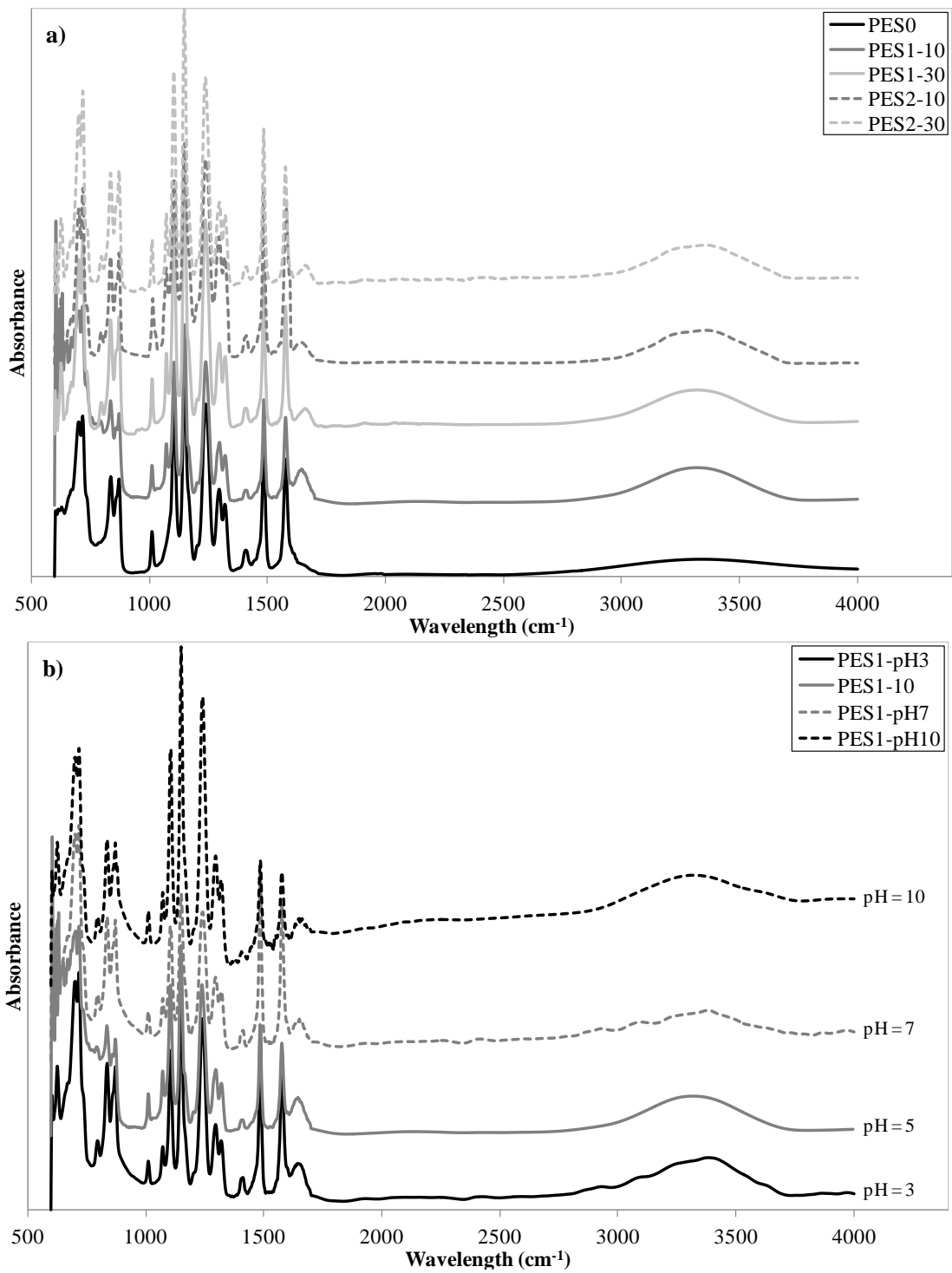


**Fig. 1.** ATR-FTIR spectra of all the membrane surfaces for different (a) irradiation time and (b) additive solution pHs.

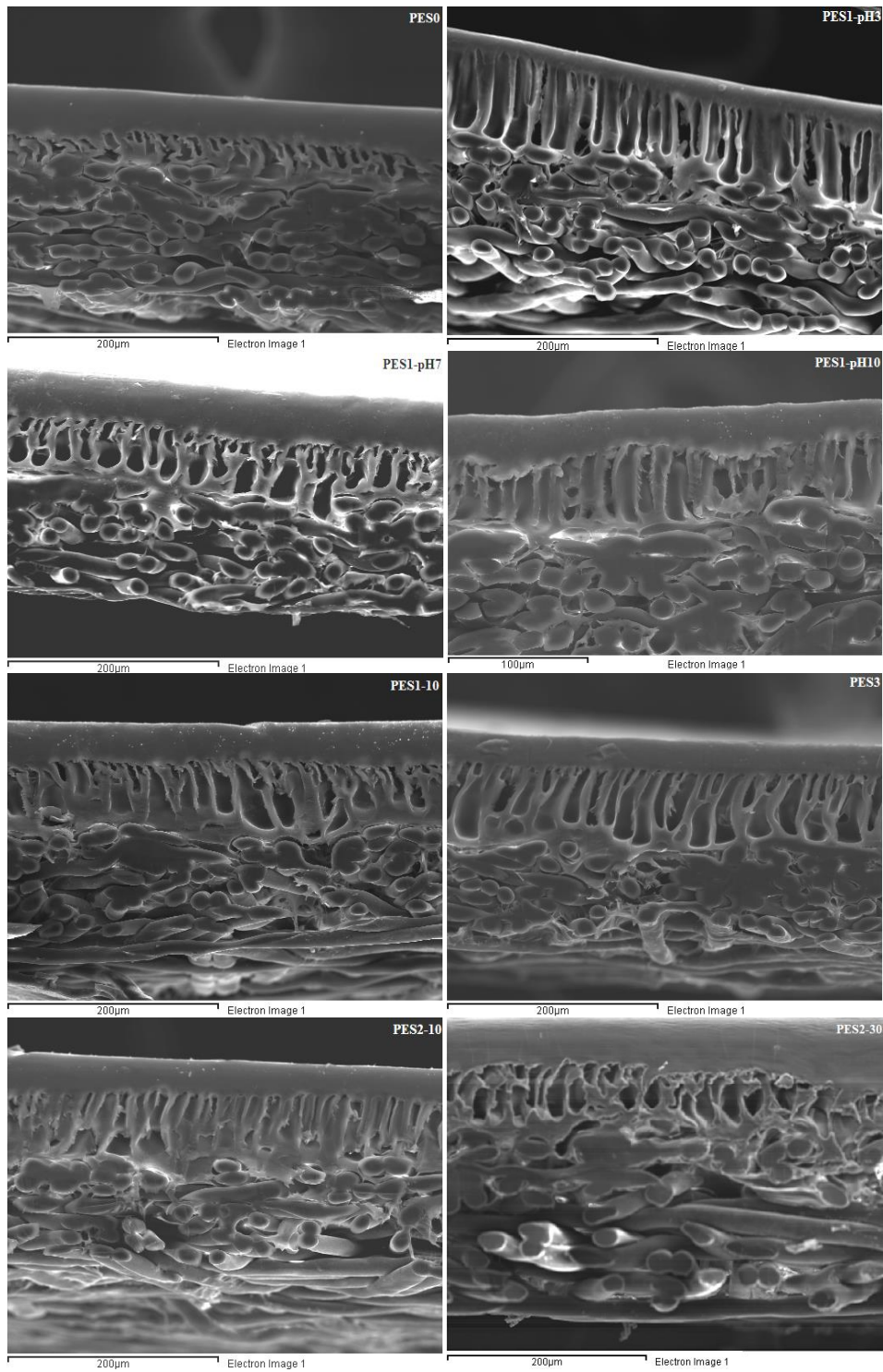


**Fig. 2.** SEM images of the cross-sections of the synthesised membranes with different PEG/ $\text{Al}_2\text{O}_3$  concentrations (PES2-10 and PES3), additive solution pHs (PES1-pH3, PES1-pH7, PES1-pH10, and PES1-10) and irradiation time (PES2-10 and PES2-30).

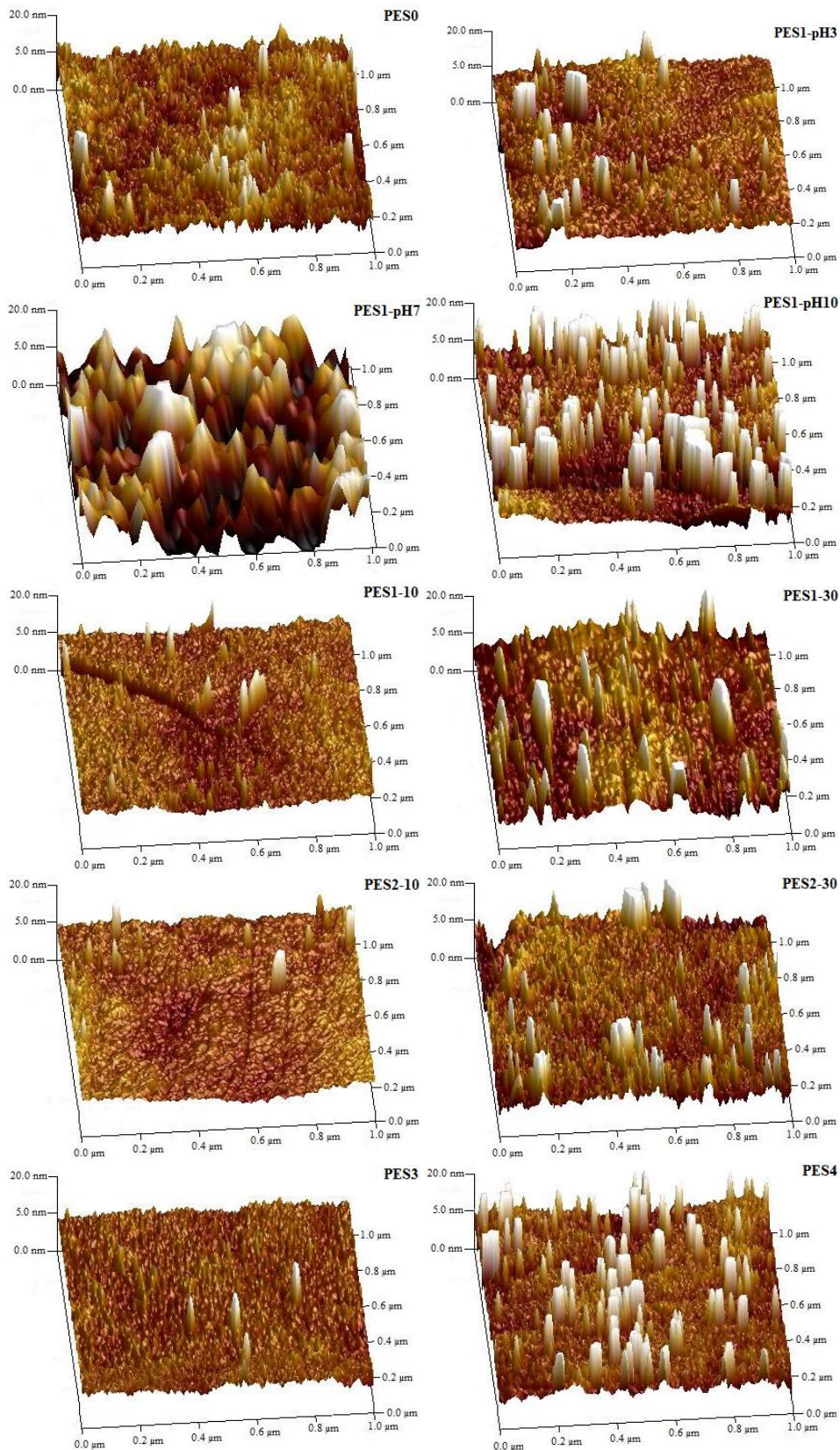


**Fig. 3.** Surface 3D AFM images of unmodified PES membrane (PES0) and PES membranes modified with different PEG/Al<sub>2</sub>O<sub>3</sub> concentrations (PES1-10, PES2-10, PES3, and PES4), additive solution pHs (PES1-pH3, PES1-pH7, PES1-pH10, and PES1-10) and incubation time (PES 1-10, PES1-30, PES2-10, and PES2-30).

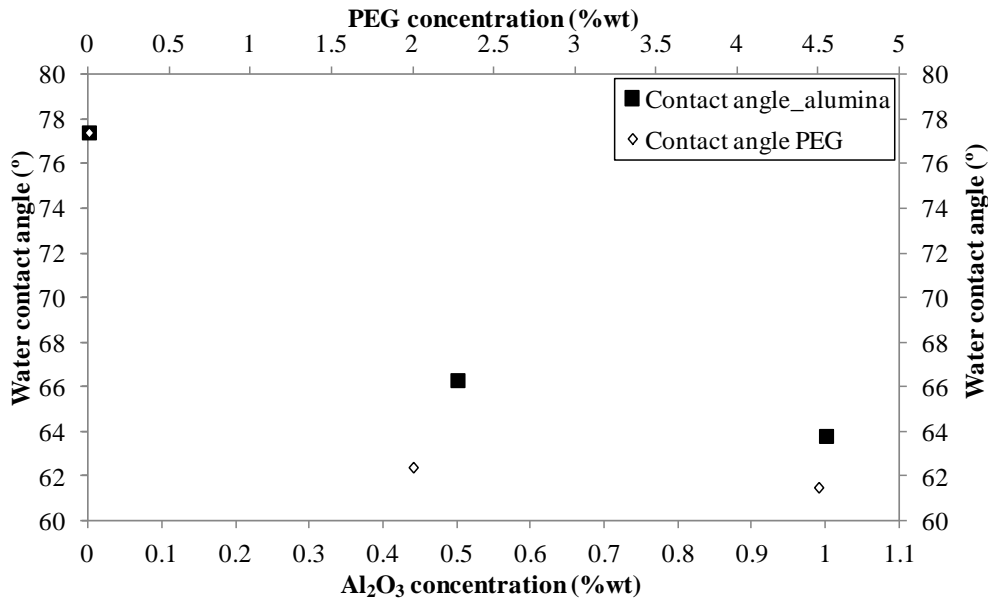


**Fig. 4.** Water contact angle values measured for different modified PES membranes at different additive concentrations.

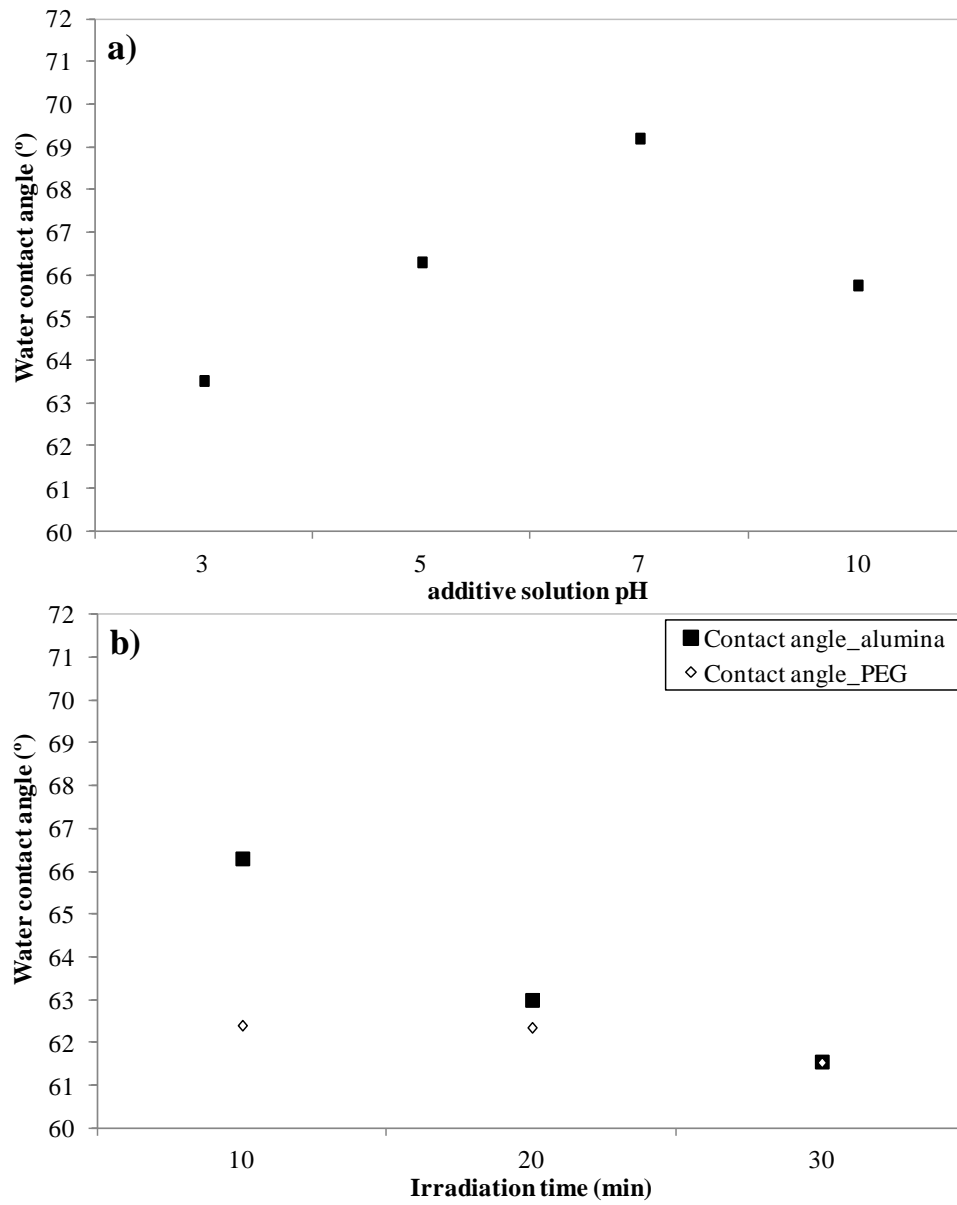


**Fig. 5.** Water contact angle values measured for different modified PES membranes at different additive solution pHs (a) and irradiation time (b).

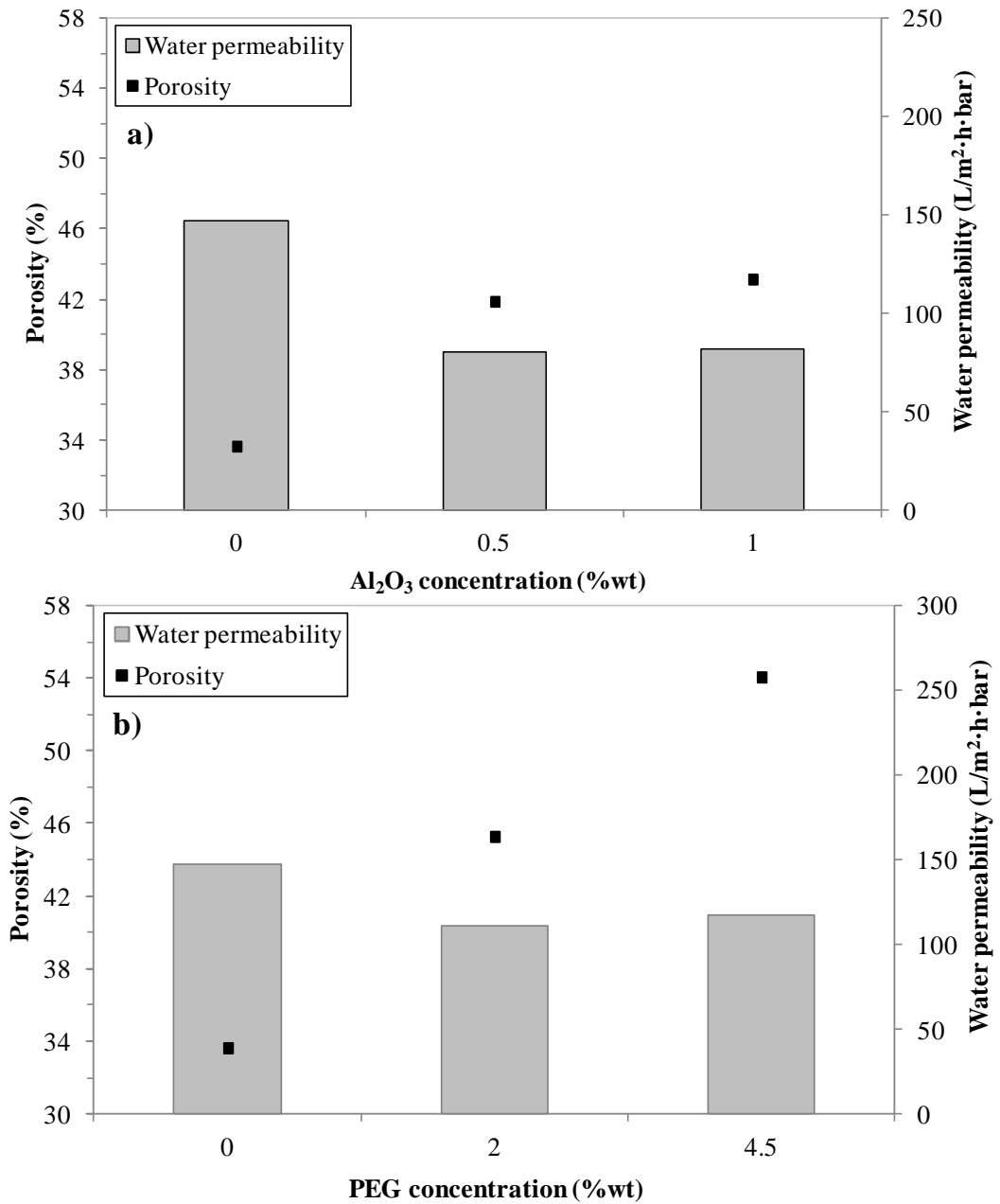


**Fig. 6.** Correlation between water permeability and porosity of the membranes with different additives concentration: (a) PES/Al<sub>2</sub>O<sub>3</sub> membranes and PES/PEG/Al<sub>2</sub>O<sub>3</sub> membranes (b).

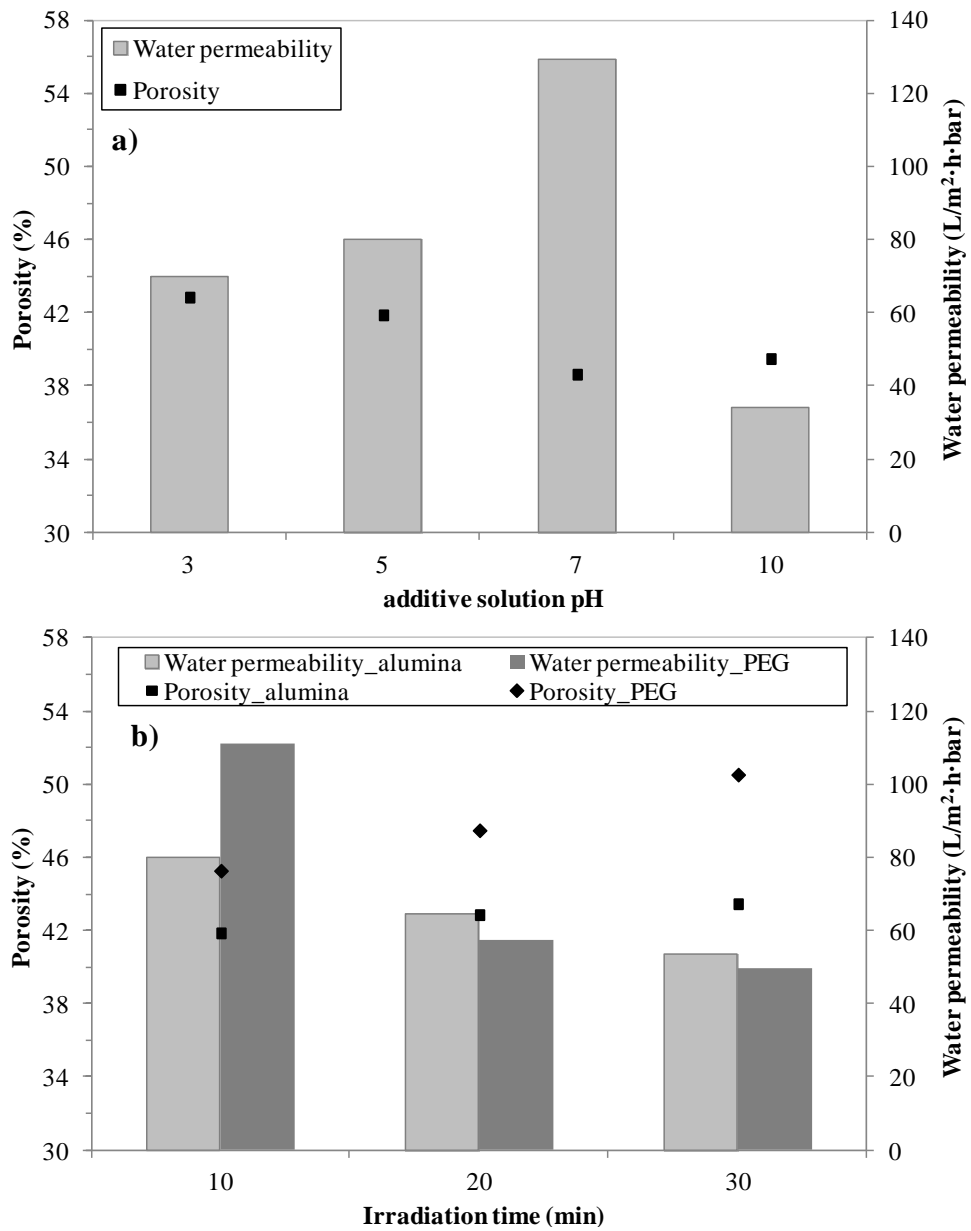


**Fig. 7.** Correlation between water permeability and porosity of the membranes at different (a) additive solution pHs and (b) irradiation times.

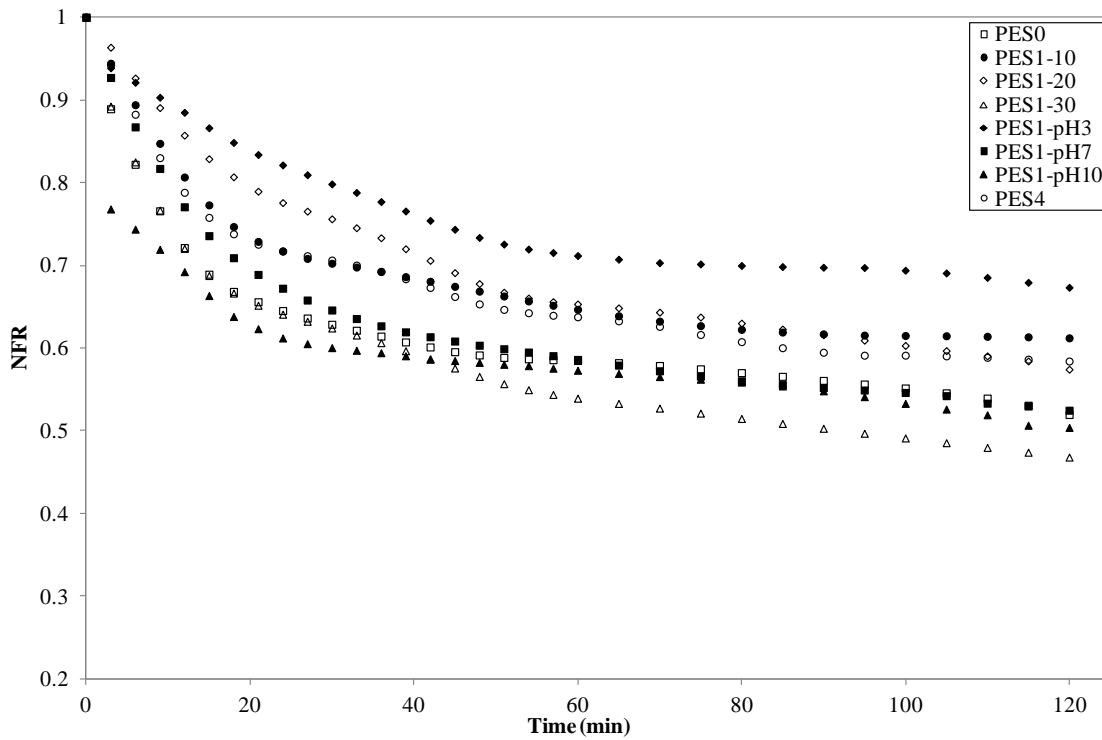


**Fig. 8.** Normalised flux ratio (NFR) in TOPW ultrafiltration of different photomodified membranes with different  $\text{Al}_2\text{O}_3$  concentrations, additive solution pH and irradiation times (25 °C, 2 bar).

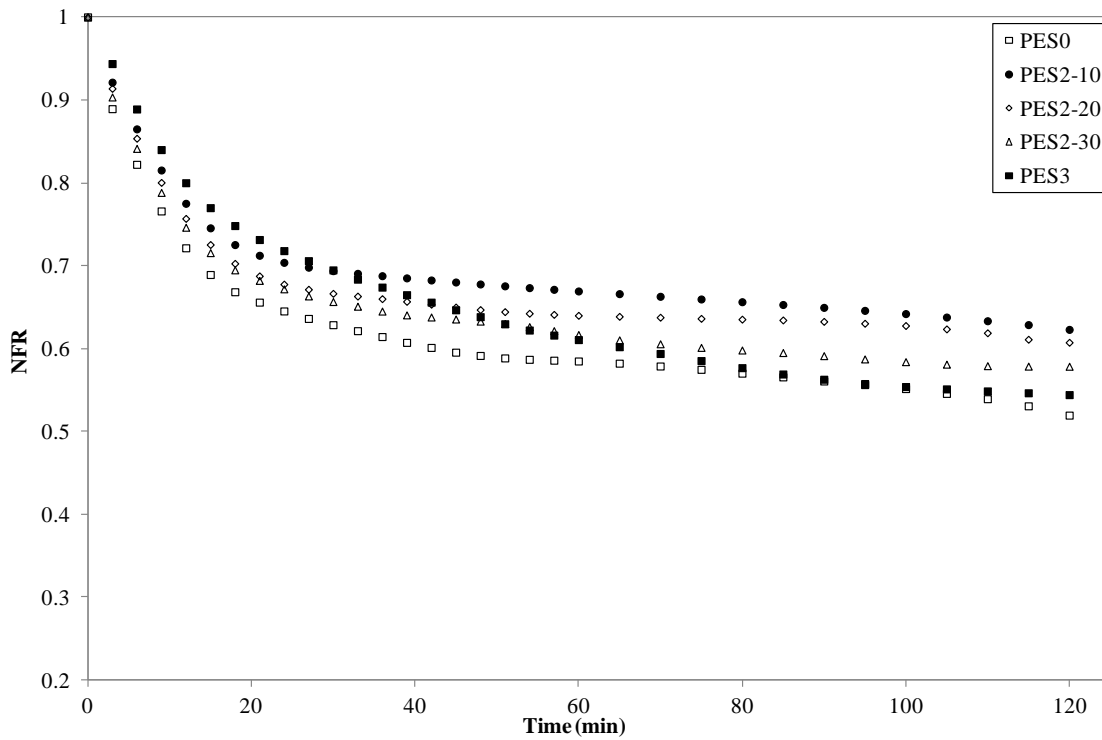


**Fig. 9.** Normalised flux ratio (NFR) in TOPW ultrafiltration of different photomodified membranes with different PEG/ $\text{Al}_2\text{O}_3$  concentrations and irradiation times (25 °C, 2 bar).

**Table 1.** Physicochemical characteristics of the wastewater used.

Parameters	Mean value
pH	4.75 ± 0.10
Electrical conductivity (mS/cm)	80.7 ± 2.0
Turbidity (NTU)	427.8 ± 4.0
COD (g of O <sub>2</sub> /L)	7.25 ± 0.26
Dry matter (g/L)	2.66 ± 0.16
Total phenolic compounds (mg of tyrosol/L)	591.1 ± 2.0

**Table 2.** Irradiation time, composition and pH of the different additive solutions used during the modification of PES membranes using UV irradiation.

Membrane	Additive composition (wt%)		additive solution pH	Irradiation time (min)
	Al <sub>2</sub> O <sub>3</sub>	PEG		
PES0	---	---	---	---
PES1-10	0.5	---	4.5-5.0	10
PES1-20	0.5	---	4.5-5.0	20
PES1-30	0.5	---	4.5-5.0	30
PES1-pH3	0.5	---	3.0	10
PES1-pH7	0.5	---	7.0	10
PES1-pH10	0.5	---	10.0	10
PES2-10	0.5	2.0	6.0	10
PES2-20	0.5	2.0	6.0	20
PES2-30	0.5	2.0	6.0	30
PES3	0.5	4.5	6.0	10
PES4	1.0	---	4.5-5.0	10

**Table 3.** Degree of modification (DM), intrinsic membrane resistance (R<sub>m</sub>), surface roughness (S<sub>a</sub>), molecular weight cut-off (MWCO) and pore size (r<sub>m</sub>) of unmodified PES membrane (PES) and all the photomodified membranes studied.

Membrane	DM (µg/cm <sup>2</sup> )	R <sub>m</sub> (·10 <sup>12</sup> m <sup>-1</sup> )	S <sub>a</sub> (nm)	MWCO (Da)	r <sub>m</sub> (nm)
PES0	---	2.797	1.1 ± 0.1	30000	5.2
PES1-10	411 ± 20	5.024	1.2 ± 0.2	26800	4.9
PES1-20	523 ± 52	6.239	2.1 ± 0.8	25200	4.7
PES1-30	599 ± 44	7.520	3.2 ± 0.7	24800	4.7
PES1-pH3	454 ± 27	5.761	1.9 ± 0.3	26000	4.8
PES1-pH7	288 ± 28	3.112	5.7 ± 0.6	26000	4.8
PES1-pH10	403 ± 30	11.828	2.6 ± 0.4	20000	4.2
PES2-10	528 ± 33	3.620	1.0 ± 0.3	29000	5.1
PES2-20	659 ± 60	7.035	1.1 ± 0.1	27000	4.9
PES2-30	708 ± 58	8.091	1.9 ± 0.2	25600	4.8
PES3	663 ± 52	3.427	1.4 ± 0.1	22500	4.4
PES4	536 ± 44	4.932	2.2 ± 0.4	21200	4.3